JOURNAL OF NANO- AND ELECTRONIC PHYSICS
Vol. **5** No 3, 03015(4pp) (2013)

ЖУРНАЛ НАНО- ТА ЕЛЕКТРОННОЇ ФІЗИКИ
Том **5** № 3, 03015(4cc) (2013)

ZnO-CdS Powder Nanocomposite: Synthesis, Structural and Optical Characterization

Dinesh Saini[1,*], R.K. Duchaniya[2]

[1] *Centre for Converging Technologies, University Of Rajasthan, J. L. N Marg, Jaipur-302055 India*
[2] *Malaviya National Institute of Technology, Jaipur-302017 India*

(Received 17 March 2013; published online 12 July 2013)

A simple mechanical alloying technique for the synthesis of ZnO-CdS powder nanocomposite is reported. Structural and optical properties of ZnO-CdS powder nanocomposite have been evaluated by suitable characterization techniques. The X-ray diffraction spectrum contains a series of peaks corresponding to reflections from various sets of lattice planes of hexagonal ZnO as well as hexagonal CdS. In UV-Vis absorption spectra, two different absorption peaks were observed. The room temperature photoluminescence spectrum of the ZnO-CdS powder nanocomposites has two emission bands: an ultraviolet emission peak at 365 nm and a green emission around 510 nm. FTIR spectroscopy confirmed the presence of Zn-O bond and Cd-S bond.

Keywords: Mechanical alloying, ZnO-CdS powder nanocomposite, X-ray diffraction, UV-Vis, Photoluminescence, FTIR.

PACS numbers: 78.67.Bf, 78.67.Sc, 62.23.Pq, 74.25.nd

1. INTRODUCTION

Nanoparticles have attracted significant interest due to their tunable electronic, optical and catalytic properties arising from the quantum confinement effect [1]. They have wide applications and uses in solar cells, light emitting devices, catalysis and bio-imaging [2]. In order to manipulate the optical properties and enhance the functionality of semiconductor nanoparticles, the field of nanocomposite materials has been widely recognized as one of the most promising and rapidly emerging research area. Promising applications are expected or have already been realized in many fields of technology such as optical and electronic materials, solid electrolytes, coating technology, sensorics, catalysis, and separation science [3]. For device applications, the nanocomposites are considered to be superior to their individual component [4].

Zinc oxide (ZnO) has shown a wide range of technological applications including UV light-emitting diodes, solar cell, field emission display, gas sensors and lasers. On the other hand, ZnO has also wide band gap energy of 3.37 eV at room temperature, which is the highest among all II-VI compounds [2]. Arrays of crystalline ZnO nanorods have been utilized as transparent electrodes in photovoltaic cells and photo electrochemical cells. However, the efficiency of such a device as a solar cell is hindered because being a wide band gap semiconductor, ZnO itself cannot absorb and utilize the visible region of the solar spectrum (> 420 nm) and less than 4 % of the solar radiation is in ultraviolet region. In order to absorb visible light and generate electron-hole pairs, it is imperative to couple the above wide band gap semiconductor with a lattice matched visible sensitizer. CdS is considered to be the most suitable visible sensitizer for ZnO because the lattice structure of CdS is same as that of ZnO, the band gap of CdS lies in the visible range and the CdS forms a type-II heterojunction with ZnO which facilitates a very fast, interband charge transfer from CdS to ZnO. The lifetime of the photogenerated carrier in ZnO-CdS composite was observed to be higher than that in the only ZnO and only CdS. The above process is responsible for an enhanced efficiency of photovoltaic cells [5, 6]. CdS has a typical wide band gap of 2.42 eV in the visible region at room temperature [2]. In this way, the above system has been a topic of greater interest for today's researchers. In this article, we report synthesis of ZnO-CdS powder nanocomposite by mechanical alloying technique followed by evaluation of their structural and optical properties by suitable techniques [6].

2. EXPERIMENTAL

2.1 Synthesis

To synthesize ZnO-CdS powder nanocomposite, ZnO nanoparticles and CdS nanoparticles were used. Both the chemicals were in powder form with hexagonal structure. In a typical experiment, to synthesize ZnO-CdS powder nanocomposite, ZnO nanoparticles and CdS nanoparticles were taken in 50 : 50 ratio in powder form as they were obtained. They were mixed by mechanical alloying method. This technique produces homogenous material starting from blended elemental powder mixtures as result of constant interplay between welding and fracturing. It gives very fine powder but with relatively coarse particle size [7].

2.2 Characterization

Various characterization techniques namely, X-ray diffraction (XRD), Scanning electron microscope (SEM), UV-Vis spectroscopy, Photoluminescence spectroscopy, and Fourier transform infrared (FTIR) measurements were employed for evaluating the performance of ZnO-CdS powder nanocomposite. All the characterizations were performed at room temperature. The dried ZnO-CdS powder was used to characterize XRD pattern. XRD pattern was obtained using Bragg-Brentanno

* dineshsatrawla@yahoo.com

geometry on P analytical X'pert Pro diffractometer in 2θ scanning range of 20°-70° with CuKα radiation source ($\lambda = 1.5406$ Å). The X-ray tube was operated at 45 kV and 40 mA. The average particle size was estimated for the major XRD peak using the Scherer equation. The optical properties of ZnO-CdS powder nanocomposite were investigated by the UV-Vis absorption spectroscopy and Photoluminescence spectroscopy. For the recording of UV-Vis absorption spectrum, ZnO-CdS powder nanocomposite was dispersed in distilled water by ultra-sonication. UV-Vis absorption spectrum was recorded on SHIMADZU UV spectrophotometer in the wavelength range 200 to 800 nm. The PL spectrum was recorded on SHIMADZU RF-5301Pc spectro photometer. The composition of the sample was estimated using Energy dispersive analysis of X-rays (EDX) attached to Scanning electron microscope (SEM, Model: ZEISS EVO 18). Fourier transform infrared (FTIR) measurements were carried out using "IR Affinity-1 SHIMADZU spectrophotometer. An FTIR spectrum of fine powdered ZnO-CdS nanocomposite was obtained in KBr powder in the range 400-4000 cm^{-1}.

3. RESULTS AND DISCUSSION

3.1 XRD Study

XRD analysis was performed to investigate the crystal phase as well as average particle size of ZnO-CdS powder nanocomposite. As shown in Fig. 1, all the diffraction peaks can be indexed as a mixture of hexagonal ZnO and the hexagonal CdS, which is well consistent with the JCPDS file Nos.-00-036-1451 and -00-006-0314, respectively. XRD peaks corresponding to the reflections from (100), (101), (102), (110) and (103) planes of hexagonal ZnO and that corresponding to the reflections from (002), (110) and (112) planes of hexagonal CdS are clearly observed in the spectrum. Any structural transformation of either ZnO or CdS was not observed. In addition, we did not observe any XRD peak corresponding to any intermediate compound formation. The obtained results were similar to that reported earlier [5, 6]. The average particle size was calculated from full width at half maximum of major XRD peaks using Debye-Scherrer's formula [8]. The average particle size of the ZnO-CdS powder nanocomposite was found ~ 78 nm.

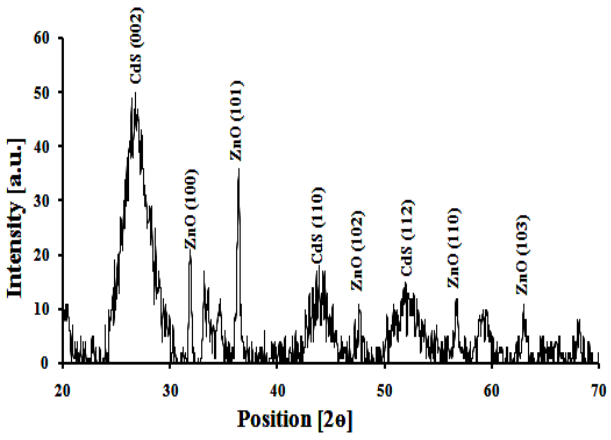

Fig. 1 – XRD spectra of ZnO-CdS powder nanocomposite

3.2 SEM Study

Fig. 2a, shows SEM image of the ZnO-CdS powder nanocomposite, which clearly indicates the formation of nanoclusters. The particles have aggregated to form clusters [9]. Individual nanoparticles are specified in red circles by black arrows. EDX pattern of ZnO-CdS powder nanocomposite is displayed in Fig. 2b, which shows separate peaks of Cadmium (Cd), Sulphur (S), Oxygen and Zinc (Zn), compositional analysis by EDX confirms that the sample is of desired composition having both the ZnO and CdS nanoparticles. EDX data shown in Table 1, gives the composition of prepared sample in weight and atomic percentage.

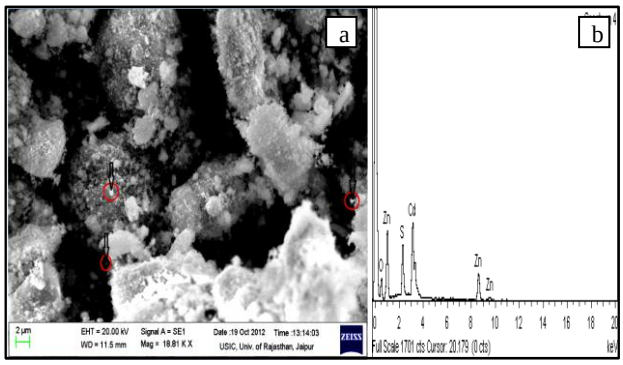

Fig. 2 – SEM image of ZnO-CdS nanocomposite (a). EDX plot of ZnO-CdS nanocomposite (b)

3.3 UV-Vis Study

In Fig. 3a, absorption spectrum of ZnO-CdS powder nanocomposite shows two peaks at 374 nm and 473 nm. The peak at 374 nm is due to ZnO nanoparticles in the composite, whereas peak at 473 nm is associated with CdS nanoparticles [10, 11]. The calculated band gap of ZnO-CdS powder nanocomposite was found 3.8 eV. The band gap of ZnO-CdS powder nanocomposites was estimated from the graph of $h\nu$ versus $(\alpha h\nu)^2$ for the absorption coefficient α that is related to the band gap E_g as $(\alpha h\nu)^2 = k((h\nu - E_g)$, where $h\nu$ is the incident light energy and k is a constant [3]. Fig. 3b shows energy band gap determination of ZnO-CdS powder nanocomposite.

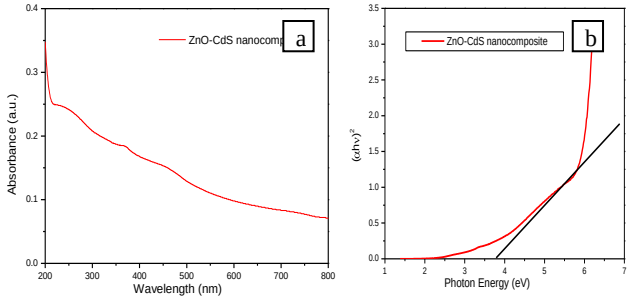

Fig. 3 – UV-Vis absorption spectra (a). Energy band gap determination (b)

3.4 PL Study

Fig. 4 shows room temperature PL spectrum of ZnO nanoparticles and ZnO-CdS powder nanocomposite for

Table 1 – Elemental analysis for ZnO-CdS powder nanocomposite

No.	Element	Weight %	Atomic %
1	O K	25.45	60.13
2	S K	9.03	10.64
3	Zn K	29.70	17.17
4	Cd L	35.83	12.05
5	Totals	100.00	100.00

comparison. The PL spectrum of ZnO nanoparticles at 275 nm excitation wavelength shows a UV-emission band at 372 nm, which is attributed to a near-band-edge transition of ZnO, namely the recombination of free excitons [12]. The PL spectrum of prepared ZnO nanoparticles is completely flat in the visible region. In this condition, ZnO cannot absorb visible light due to its wide band gap, which is not favourable for solar cell applications. Whereas, the PL spectrum of ZnO-CdS powder nanocomposite at 300 nm excitation wavelength presents two emission bands: A UV-emission band at 365 nm and a broad Green emission band centered at 510 nm. In comparison with ZnO nanoparticles, the ZnO-CdS powder nanocomposite shows a small (~ 7 nm) blue shift in UV region and a large (~ 42 nm) red shift in the visible region. According to the structural characteristics of the ZnO-CdS powder nanocomposites, both the blue shift and the red shift in the PL spectrum could be attributed to the interaction between the two semiconductors of ZnO and CdS [13]. The band in visible range may be associated with sulfur and oxygen states and the high intensity can be due to collaborative effect of ZnO and CdS nanoparticles. So it is clear that for ZnO-CdS powder nanocomposite, there is a drastic change in the nature of PL spectra (large red shift in visible region). In this case, the sensitization of ZnO for visible light will be increased. Hence, the obtained PL is desirable for solar cell applications.

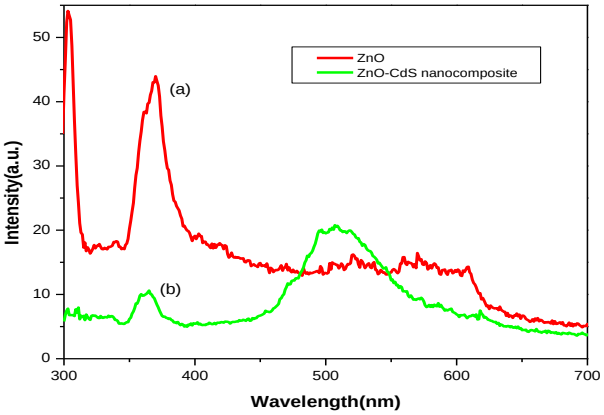

Fig. 4 – PL spectrum of ZnO-CdS powder nanocomposite

3.5 FTIR Study

Fig. 5 shows the FTIR spectrum of ZnO-CdS powder nanocomposite in the frequency range (400-4000 cm^{-1}). The band located at 460 cm^{-1} is correlated to metal oxide bond (Zn-O), which confirms the formation of ZnO [14]. There is a band at 644 cm^{-1} is due to the stretching frequency of Cd-S bond [15]. The band at 1340 cm^{-1} and 1404 cm^{-1} corresponds to the C = O bending vibrations and C = O stretching vibrations respectively [16]. The peak at 1610 cm^{-1} is associated with O-H bending vibrations of H_2O [9, 15]. The band located near 2353 cm^{-1} can be attributed to the C = O residue probably due to atmospheric CO_2 [12]. A broad peak in the range of 3200 cm^{-1} to 3500 cm^{-1} corresponds to the vibrational mode of O-H bond [16].

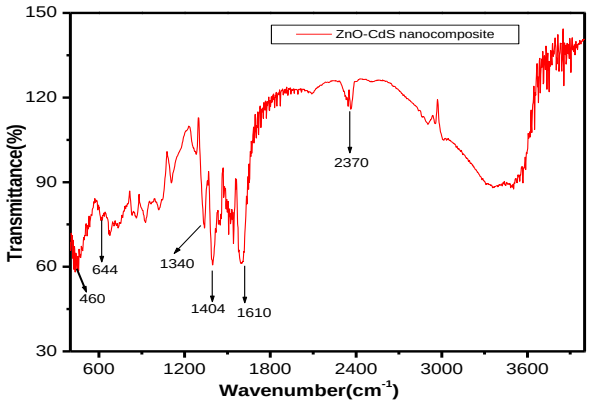

Fig. 5 – FTIR spectrum of ZnO-CdS powder nanocomposite

4. CONCLUSION

ZnO-CdS powder nanocomposite was successfully synthesized via simple mechanical alloying method. The average particles size calculated by XRD analysis was found 78 nm. SEM data showed the agglomerated form of nanoparticles. The EDX spectra showing that the powders are stoichiometric compositions. The band gap was obtained by UV-Vis spectroscopy. Photoluminescence spectra indicated large red shift in the visible region. In FTIR, it confirms the successful synthesis of ZnO-CdS powder nanocomposite due to the existence of peaks of both Zn-O bond and Cd-S bond. The synthesized nanocomposite would be potentially useful for solar cell applications.

ACKNOWLEDGEMENTS

Authors thankfully acknowledge to University Of Rajasthan, Jaipur for this work and Mr.Manoj Jangid & Mr. Ravi Agarwal for technical support.

REFERENCES

1. S.K. Panda, S. Chakrabarti, B. Satpati, P.V. Satyam, S. Chaudhuri, *J. Phys. D: Appl. Phys.* **37**, 628 (2004).
2. G. Murugadoss, *J. Lumin.* **132**, 2665 (2012).
3. Litty Irimpan, V.P.N. Nampoori, P. Radhakrishnan, *J. Appl. Phys.* **103**, 094914 (2008).
4. J. Nayak, S.N. Sahu, J. Kasuya, S. Nozaki, *Appl. Surf. Sci.* **254**, 7215 (2008).
5. J. Nayak, H. Lohani, T.K. Bera, *Curr. Appl. Phys.* **11**, 93 (2011).
6. J. Nayak, Min-Kyu Son, Jin-Kyoung Kim, Soo-Kyoung Kim, Jeong Hoon Lee, Hee Je Kim, *J. Electr. Eng. Technol.* **7** No. 6, 965 (2012).
7. C. Suryanarayana, *Prog. Mater. Sci.* **46**, 1 (2001).
8. G. Murugadoss, *Appl. Nanosci.* (November 2012).
9. B. Srinivasa Rao, B. Rajesh Kumar, V. Rajagopal Reddy, T. Subba Rao, *Chalcogenide Lett.* **8**, **177** (2011).
10. Yong-Hong Ni, Xian-Wen Wei, Jian-Ming Hong, Yin Ye, *Mater. Sci. Eng. B* **121**, 42 (2005).
11. Rajeev R. Prabhu, M. Abdul Khadar, *PRAMANA-J. Phys.* **65** No. 5, 801 (2005).
12. Chira R. Bhattacharjee, Debraj Dhar Purkayastha, Sumit Bhattacharjee, Abhijit Nath, *Phys. Sci. Technol.* **7**, 122 (2011).
13. Tao Gao, Qiuhong Li, Taihong Wang, *Chem. Mater.* **17**, 887 (2005).
14. R.Y. Hong, J.H. Li, L.L. Chen, D.Q. Liu, H.Z. Li, Y. Zheng, J. Ding, *Powder Technol.* **189**, 426 (2009).
15. Aurobinda Acharya, Rajkishore Mishra, G.S. Roy, *Lat. Am. J. Phys. Educ.* **4** No. 3, 603 (2010).
16. S. Zandi, P. Kameli, H. Salamati, H. Ahmadvand, M. Hakimi, *Physica B* **406**, 3215 (2011).